

Synthesis of a novel smectic liquid crystalline glass and characterization of its charge carrier transport properties†

Jiang Wu,^a Takayuki Usui^b and Jun-ichi Hanna^{*ab}

Received 1st March 2011, Accepted 5th April 2011

DOI: 10.1039/c1jm10890e

A new organic semiconductor material with both a self-organized molecular alignment in smectic liquid crystals and a solid nature in amorphous materials, *i.e.*, a glassy liquid crystalline organic semiconductor has been proposed, and its model compound, 1,3,5-benzenetricarboxylic acid, tris{12-[6'-(4''-octylphenyl)-2'-naphthyl-1-dodecyl ester]} (LCG-triester 8-PNP-O12), was synthesized, and we characterized its phase transition behaviors in slow cooling and rapid cooling. It exhibited smectic A (SmA) and smectic B (SmB_{hex}) phases in slow cooling, and a SmB_{hex} glassy phase with a high T_g close to 60 °C when cooled rapidly from the SmA and SmB_{hex} phases. Its charge carrier transport properties in the smectic mesophases, including the liquid crystal glassy phase, were first studied by the time-of-flight (TOF) technique, which revealed that the hole mobility in the SmB_{hex} glassy phase was about $3.5 \times 10^{-4} \text{ cm}^2 \text{ v}^{-1} \text{ s}^{-1}$, comparable to that in the SmB_{hex} liquid crystal phase. We concluded that the high charge transport properties of the smectic mesophase are successfully maintained in the solid glassy state.

Introduction

In the past decades, amorphous films of organic photoconductors, including molecularly doped polymers, *e.g.*, triarylamine derivatives, dispersed in a polymer matrix have been used as important components of photoreceptors for electrophotographic copiers and laser printers.¹ Their application has been extended for charge transport layers for organic light emitting diodes (OLEDs).² In these amorphous materials, which are characterized as molecular aggregates without any orientational or positional order, charge transport properties are described by hopping conduction in energetically and spatially distributed localized states consisting of aromatic molecular moieties of the materials.³ Therefore, the mobility is strongly field and temperature dependent, and is typically in the order of 10^{-6} to $10^{-5} \text{ cm}^2 \text{ v}^{-1} \text{ s}^{-1}$.^{4,5} This mobility is 6 orders of magnitude smaller than that of their single crystals, in which all the molecules are closely packed in a crystal lattice and aligned in a long-range order and the charge carrier transport properties are described by the band conduction, especially at low temperatures.^{6,7} Because of the high mobility of around $0.5 \text{ cm}^2 \text{ v}^{-1} \text{ s}^{-1}$ in organic

polycrystalline thin films, which is comparable to that of amorphous silicon—used for TFT arrays for liquid crystal displays, renewed attention has been focused on organic polycrystalline thin films for TFT applications such as e-papers and radio frequency identification (RFID) tags.

On the other hand, there has also been considerable interest in carrier transport properties in liquid crystals,^{8–14} which comes from the basic idea that the molecular alignment of liquid crystals should be beneficial to the fast carrier transport.¹⁵ In fact, the charge carrier transport properties of discotic hexagonal liquid crystalline phases (D_h) of phthalocyanine and porphyrin derivatives were studied by microwave conductivity measurement.¹⁶

In the 1990s, the electronic conduction was established in both the discotic columnar phase of hexakis n-pentyloxy-triphenylene^{17,18} and a smectic phase of 2-phenylbenzothiazole derivatives, these discoveries gave us a new insight into the fact that the liquid crystal is a new type of organic semiconductor exhibiting self-organization and a high mobility over $10^{-3} \text{ cm}^2 \text{ v}^{-1} \text{ s}^{-1}$.^{19,20} Indeed, liquid crystalline materials are quite attractive as an organic semiconductor because of their high mobility, which is superior to amorphous materials,²¹ easy control of the molecular orientation²² and their electrically less active domain boundaries and disclinations²³ which are superior to polycrystalline materials. Thus, we have investigated the charge carrier transport properties in various liquid crystals in order to establish their firm basis for industrial applications to organic devices after the discovery of their electronic conduction in the smectic mesophases.^{24,25}

However, there remain a few questions to be answered about the charge carrier transport properties in the liquid crystals: how

^aImaging Science and Engineering Laboratory, Tokyo Institute of Technology, Nagatsuta, Midori-ku, Yokohama, 226-8503, Japan. E-mail: hanna@isl.titech.ac.jp; Fax: +81-45-924-5176; Tel: +81-45-924-5176

^bJST-CREST, Kawaguchi, Saitama, Japan

† Electronic supplementary information (ESI) available: sample preparations for TOF measurement are shown in Figs. 1 & 2. The TOF experimental setup is shown in Fig. 3. The molecular alignment in liquid crystal cell is described in Fig. 4. See DOI: 10.1039/c1jm10890e

does the molecular disorder, which is caused as a result of molecular motion in a liquid-like phase, affect the charge carrier transport in the mesophases? How does the dynamic motion of the molecules affect it? Thus, we are interested in a new material that has molecular alignment in the liquid crystal mesophase and frozen molecular motion, *i.e.*, a liquid crystal glass (LCG). Bearing this in mind, we have designed a smectic liquid crystal glass based on a 2-phenylnaphthalene derivative as a model.

In this report, we describe the design and synthesis of the new smectic glass and its phase transition behavior, in addition to preliminary results on its charge carrier transport properties.

Material design

Liquid crystal mesophases have a higher degree of sophistication in the molecular order than amorphous glasses, where all the molecules sit randomly without any molecular orientational or positional order, so they crystallize easily when the temperature goes down, particularly small molecules. Therefore, we need a subsidiary structure to suppress the crystallization and induce a smectic glassy phase, except for nematic glasses of π -conjugated main chain polymers and oligomers. In fact, the dimer structure was introduced in order to have a glassy columnar mesophase in a triphenylene derivative,²⁶ and a trimer structure for a nematic glassy phase in a triester of 1,3,5-benzenetricarboxylic acid.²⁷

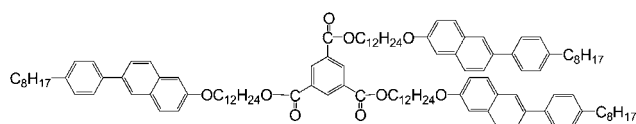
Thus, we adopted a trimer structure based on benzene tricarbonylic acid as the subsidiary structure unit and the 2-(4'-octylphenyl)-6-dodecyloxy-naphthalene (8-PNP-O12) moiety as a mesogen unit for a model material, 1,3,5-benzenetricarboxylic acid, tris{12-[6'-(4''-octylphenyl)-2'-naphthylloxy]-1-dodecyl ester} (LCG-triester 8-PNP-O12), shown in Scheme 1.

Experimental

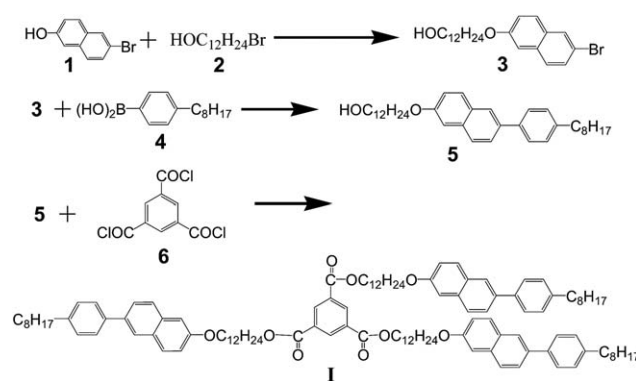
1. Material synthesis

All the solvent and reagents were obtained from Tokyo Chemical Industry. Co. Ltd or Sigma-Aldrich Chemical Co., and used without further purification. Compounds **1** and **2** were purchased. Compounds **3**²⁸ and **5**²⁹ were prepared by following the literature. Our model compound, LCG-triester 8-PNP-O12 (**I**) was prepared from the ester condensation of benzene tricarbonylic chloride with an alcohol of 8-PNP-O12, as shown in the Scheme 2. The isolated product (**I**) was purified carefully by flash column chromatography and recrystallized from dichloroform. All ¹H and ¹³C NMR were measured on JEOL-JNM-WinL α -500 and HRMS were measured on a Bruker micro TOFII at ESI mode.

12-[6-(4-octylphenyl)-2-naphthylloxy]-1-dodecanol (5). A biphasic mixture of toluene (11 mL), and a 2 M sodium



Scheme 1 The molecular structure of LCG-triester 8-PNP-O12.



Scheme 2 Synthetic route of LCG-triester 8-PNP-O12 (**I**).

carbonate solution (3 mL) was purged with argon gas before adding 4-octylphenylboronic acid (737 mg, 3.15 mmol), compound **3** (1143 mg, 3 mmol) and tetrakis(triphenyl-phosphine)palladium(0) (104 mg, 0.09 mmol). The reaction mixture was heated to 100 °C under argon for 6 h and the aqueous layer was extracted by CHCl_3 . The combined organic layers were washed with water, dried over MgSO_4 and filtered. The filtrate was evaporated and the crude product was purified by column chromatography (silica gel) using CHCl_3 ($R_f = 0.4$) as an eluent, followed by recrystallization from hexane to give **5** as a colorless crystal (774 mg, 50% yield).

¹H NMR (500 MHz, CDCl_3 , TMS), δ (ppm) = 7.12–7.97 (m, 10H), 4.07 (t, 2H), 3.63 (t, 2H), 2.65 (t, 2H), 1.97 (quint, 2H), 1.82 (quint, 2H), 1.63 (quint, 2H), 1.20–1.50 (m, 26H), 0.88 (t, 3H). ¹³C NMR (125 MHz, CDCl_3 , TMS), δ (ppm) = 157.19, 141.89, 138.55, 136.25, 133.70, 129.16, 128.88, 127.11, 127.01, 125.94, 125.27, 119.38, 106.45, 68.09, 63.09, 35.64, 32.83, 31.91, 31.53, 29.61, 29.58, 29.52, 29.44, 29.43, 29.41, 29.29, 26.13, 25.75, 22.69, 14.10.

ESI-TOF-MS: Calcd. For $\text{C}_{36}\text{H}_{52}\text{O}_2$ [$\text{M}]^+$: 516.3857; Found: 516.3860.

1,3,5-benzenetricarboxylic acid, tris{12-[6'-(4''-octylphenyl)-2'-naphthylloxy]-1-dodecyl ester} (I**).** A solution of 1,3,5-benzenetricarbonyl trichloride (46 mg, 0.175 mmol), compound **5** (280 mg, 0.543 mmol), and 4-dimethylaminopyridine (DMAP) (86 mg, 0.706 mmol) in 20 mL of anhydrous dichloroethane was heated at 60 °C for 3 h. The reaction mixture was then poured into cold water. The precipitate was filtered and dried in a vacuum oven. Further purification was accomplished by silica gel column chromatography, with CHCl_3 ($R_f = 0.5$) as the eluent, followed by recrystallization from dichloromethane to give **I** as a colorless solid (147 mg, 49% yield).

¹H NMR (500 MHz, CDCl_3 , TMS), δ (ppm) = 8.84 (s, 3H), 7.12–7.95 (m, 30H), 4.36 (t, 6H), 4.06 (t, 6H), 2.65 (t, 6H), 1.83 (quint, 6H), 1.78 (quint, 6H), 1.65 (quint, 6H), 1.20–1.50 (m, 78H), 0.88 (t, 9H). ¹³C NMR (125 MHz, CDCl_3 , TMS), δ (ppm) = 165.12, 157.13, 141.86, 138.48, 136.17, 134.41, 133.64, 131.47, 129.54, 129.09, 128.86, 127.09, 126.98, 125.91, 125.24, 119.36, 106.30, 68.02, 65.85, 35.63, 31.90, 31.55, 29.58, 29.51, 29.41, 29.29, 29.27, 29.26, 28.65, 26.12, 25.98, 22.68, 14.12.

ESI-TOF-MS: Calcd. For $\text{C}_{117}\text{H}_{156}\text{O}_9$ [$\text{M}]^+$: 1705.1596; Found: 1705.1642.

2. Measurements

The phase transition behavior was determined by differential scanning calorimetry (DSC, Seiko Inst. DSC 5400C) experiments calibrated with standard samples of indium.

The polarizing optical microscopy (POM) study was carried out on a Nikon optical polarizing microscope equipped with a Mettler Toledo FP900 hot stage. Each powder-like sample was placed on a glass slide and covered with another glass cover slip.

The X-ray diffractometry (XRD) experiment was carried out on a Rigaku RAD-2B to identify the phase structure at different temperatures.

Transient photocurrents were measured by a time-of-flight (TOF) technique with an N₂ pulse laser for photoexcitation. Briefly, the compound was filled by capillary action into a liquid crystal cell which was pre-coated by indium tin oxide (ITO) as the electrode. A DC power supply was used to provide the necessary bias voltage to the sample for the relevant carrier detection. A N₂ laser ($\lambda = 337$ nm, pulse duration = 600 ps) was used for the photogeneration of free charges near one side of the sample, and the resulting transient photocurrent was recorded in a digital oscilloscope (Nicolet Accura 100). A current sensing resistor R in series with the sample for converting and magnifying the photocurrent to voltage readings was adjusted between 1 and 1 M Ω so that the RC time constant should be at least 20 times less than the carrier transient time in order to suppress distortion of the transient photocurrent.

Results and discussion

Thermotropic property

The phase transition temperature of LCG-triester 8-PNP-O12 was studied by DSC measurement, as shown in Fig. 1 and Fig. 2.

In the slow cooling with a rate of 5 °C min⁻¹, there were two mesophases from 131 to 106 °C and from 106 to 77 °C, respectively, which was shown in Fig. 1. Judging from the heat capacity at these transitions, the two mesophases are smectic phases, which are identified as smectic A (SmA) and SmB_{hex} phases by the XRD measurement described later on. In the slow heating cycle, it does not show any mesophase transition and crystallized

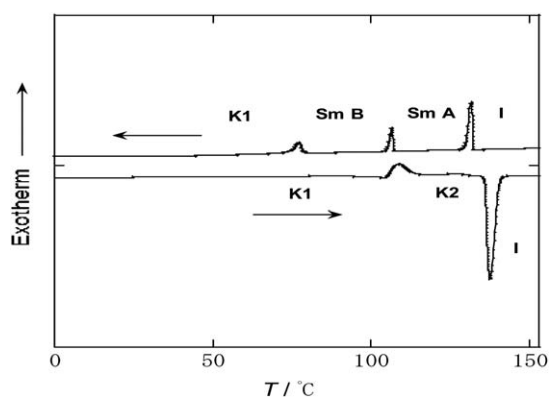


Fig. 1 DSC traces of LCG-triester 8-PNP-O12 under slow cooling and heating at 5 °C min⁻¹. Symbols: SmA; smectic A phase; SmB: smectic B phase; K: crystal phase; I: isotropic phase.

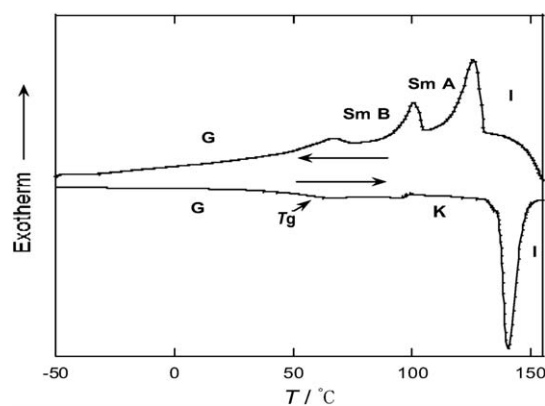


Fig. 2 DSC traces of LCG-triester 8-PNP-O12 under fast cooling and heating at 40 °C min⁻¹. Symbols: T_g : glass transition temperature; G: glassy state; SmA; smectic A phase; SmB: smectic B phase; K: crystal phase; I: isotropic phase.

near 108 °C, followed by melting into an isotropic liquid at 138 °C.

On the other hand, if we treated this sample with different cooling rates, we observed different phase transition behaviors. For fast cooling with a rate of 40 °C min⁻¹ from the isotropic phase, there also are two mesophases, from 127 to 101 °C and from 101 to 68 °C, which was shown in Fig. 2. These phases correspond to the two smectic mesophases described above. By continuously cooling the sample at a high rate of 40 °C min⁻¹, it was frozen into the glass state without crystallization. A second order transition obtained for the heating run at approximately 60 °C shows a small change in the heat capacity C_p for the glass transition, crystallization near 100 °C and melting into an isotropic liquid at 140 °C.

We also studied the phase transition behaviors of its corresponding monomer, 2-(4'-octylphenyl)-6-dodecyloxy-naphthalene (8-PNP-O12), which exhibits an SmA and SmB_{hex} liquid crystalline phase between 79 and 100 °C, 100 and 121 °C, respectively,³⁰ although no glass behavior was observed in this monomer. However, the LCG-triester 8-PNP-O12, in which the mesogenic pendant 2-phenyl naphthalene was chemically bonded to a central core, is able to form a glass state and is morphological stable for over two years under ambient atmosphere.

Optical texture and phase identification

As the results of DSC measurement, LCG-triester 8-PNP-O12 exhibits two mesophases when it was cooled from isotropic liquid. To realize the texture in each phase, we loaded it into a liquid crystal cell and observed its texture under POM, as shown in Fig. 3.

Firstly, we melted the material to the isotropic phase by Mettler Toledo FP900 hot stage with an accuracy of 1 K, and then cooled it to room temperature at different cooling rates. Fig. 3(a) shows a POM image at 120 °C. It exhibits a focal conic defect with a fan-like texture for the SmA phase, which is a typical so-called smectic texture. (b) is the following smectic mesophase at 90 °C not showing any big changes in the texture. When we quenched the sample from 90 °C to room temperature, we got a glassy phase without encountering crystallization (c),

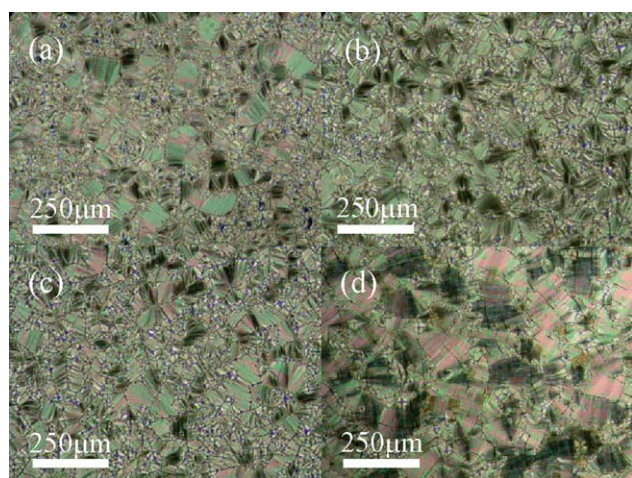


Fig. 3 (a) POM image of LCG-triester 8-PNP-O12 loaded into a liquid crystal cell at 120 °C. (b) POM image at 90 °C. (c) POM image at 25 °C by fast cooling. (d) POM image at 25 °C by slow cooling.

it is clear that the texture was almost the same as in (b), which indicated that the texture was successfully kept unchanged through glass transition. However, if we cooled the sample slowly with a cooling rate of 1 °C min⁻¹, the sample became crystallized and exhibit clear cracks among grains (d).

The phase structures were also examined by an X-ray diffraction study (XRD) at different temperatures, as shown in Fig. 4. For (a), the broad diffraction peak at the high diffraction angle region reveals that the mesophase at 120 °C is a SmA phase. For (b), A sharp diffraction peak at 19.2° with a lattice constant of 4.6 Å indicates the existence of a hexagonal lattice in the mesophase at 90 °C, which is a typical pattern for a SmB_{hex} liquid crystal phase. By quenching the sample to room temperature from the SmB_{hex} phase, it formed a glassy state and the XRD pattern was shown in Fig. 4(c), where a relatively sharp diffraction peak exits at 19.5°. The molecular alignment in the SmB_{hex} phase was well maintained in the solid state, *i.e.*, a glassy state of SmB_{hex}. We tried to form isotropic and SmA glassy states by cooling the cell from either isotropic or SmA phases at various cooling rates up to 500 °C min⁻¹. However, all the trials resulted in the SmB_{hex} glassy state. It is worth noting that only the SmB_{hex} glassy state appeared when rapidly cooled, irrespective of cooling rates. This suggests the possible appearance of even higher ordered smectic glassy states in a better structure of liquid crystals.

On the other hand, when the sample was cooled very slowly from the SmB_{hex} phase to room temperature, the sample crystallized to form a polycrystal with an XRD pattern, as shown in (d).

To the best of our knowledge, this is the first example of glassy SmB_{hex}. The glassy SmA phase was reported elsewhere.³¹

Charge carrier transport properties

In order to characterize the charge carrier transport properties of LCG-triester 8-PNP-O12, transient photocurrents were measured by TOF experiments. The LCG-triester 8-PNP-O12 was placed between two glass plates which were precoated with

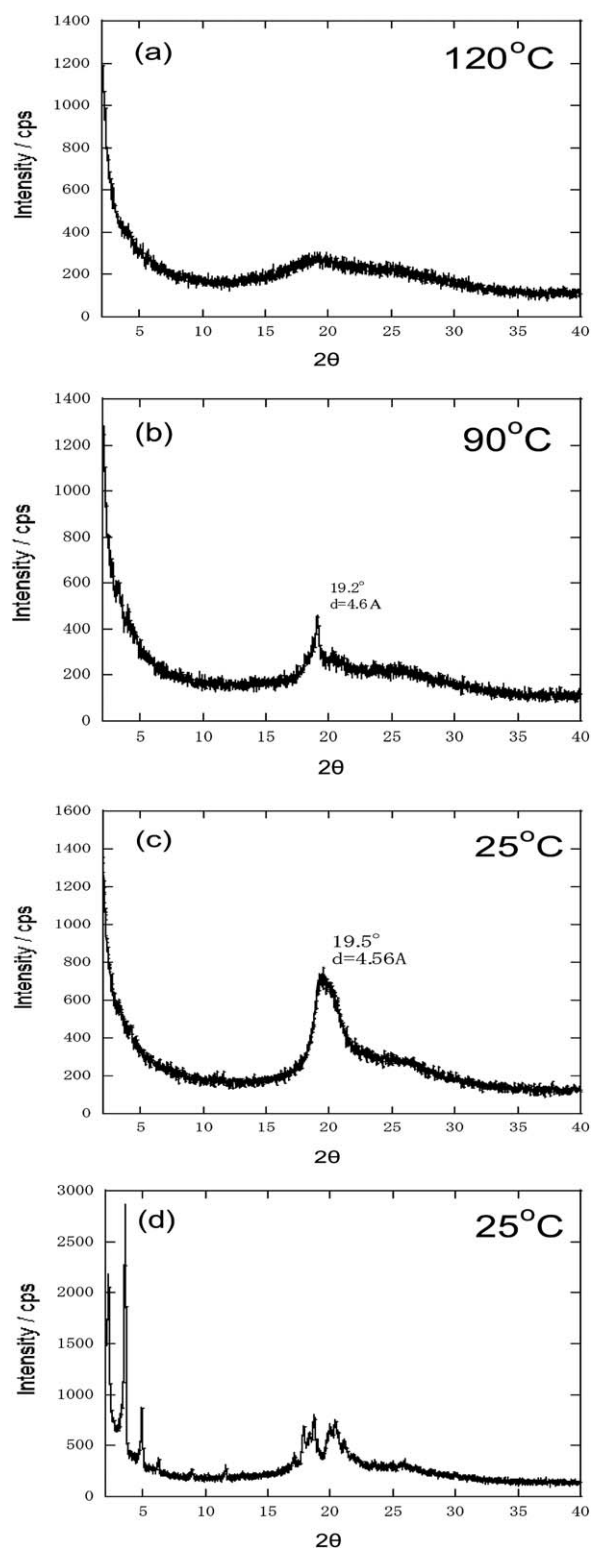


Fig. 4 XRD patterns of LCG-triester 8-PNP-O12 (a) at 120 °C, (b) at 90 °C, (c) at 25 °C by fast cooling. (d) at 25 °C by slow cooling.

ITO electrodes. The resulting cell showed planar alignment where the long axis of the pendant moiety of 2-phenyl-naphthalene is planar to the glass surface (see ESI†). The thickness of the cell was 15 μm. Pulsed (600 ps) nitrogen laser

irradiation (337 nm wavelength) in the absorption band of the LCG-triester 8-PNP-O12 leads to the generation of free electrons and holes in the electrically biased cell. Depending upon the polarity of the external electric field, electrons or holes will drift across the sample cell, causing displacement currents which can be recorded in an external circuit as shown in Fig. 5. For details of the sample preparation and of the experimental setup see ESI.†

Transient photocurrents for hole transport of LCG-triester 8-PNP-O12 in SmA and SmB_{hex} phase are shown in Fig. 5. We could not observe any transient photocurrent attributed to the drift of photogenerated negative charges, *i.e.*, electron transport. Judging from the constant photocurrent before transit time and its simple decay down to a few ms shown in the inset of Fig. 5(a) for the SmA phase, the LCG-triester 8-PNP-O12 is highly purified and the concentration of electrically active impurities in it is quite small, *i.e.*, less than a few ppm.^{32,33} All the transient currents in Fig. 5 are so-called “non-dispersive”, where the dispersion of carrier velocity is very small, so that the transit time, t_T , can be well defined and easily determined from a shoulder in each photocurrent.

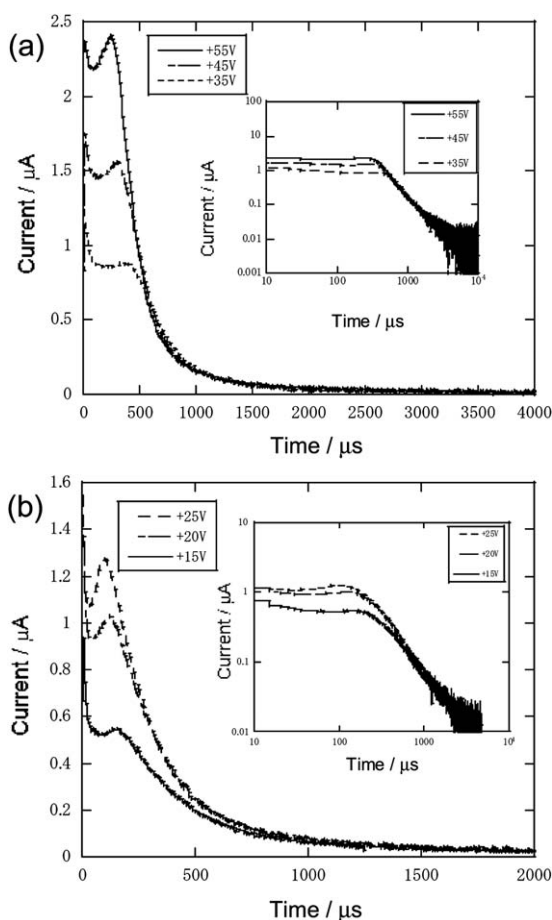


Fig. 5 Transient photocurrent of hole transport (a) in SmA phase (120 °C); (b) in SmB phase (80 °C) of LCG-triester 8-PNP-O12 in a 15 μm thick glass cell precoated by an ITO electrode at various applied voltages. The inset is the double logarithmic plot of respective transient photocurrents as a function of time.

The charge carrier mobility μ , which characterizes the macroscopic charge transport properties, is calculated by the well-known eqn (1), where d is the sample thickness and E is the electric field, V is a given applied voltage and t_T is the transit time.

$$\mu = \frac{d}{Et_T} = \frac{d^2}{Vt_T} \quad (1)$$

On the other hand, the initial photocurrent goes down sharply after illumination by a light pulse and then the current increases before the transit time again. This is probably due to charges trapped at the interface of the electrode and the thermal detrapping of trapped charges at the trap states. The hole mobility of SmA and SmB_{hex} phase is determined to be $1.25 \times 10^{-4} \text{ cm}^2 \text{ V}^{-1} \text{ s}^{-1}$ and $5 \times 10^{-4} \text{ cm}^2 \text{ V}^{-1} \text{ s}^{-1}$ at 25 V, respectively. The mobility in the SmB_{hex} phase is about 4 times higher than that for the SmA phase, which is attributed to the higher molecular alignment *i.e.*, shorter intermolecular distance in the SmB phase, supported by XRD study.

Fig. 6(a) shows transient photocurrents of holes in the SmB_{hex} glassy phase (55 °C) which was formed by rapid cooling from

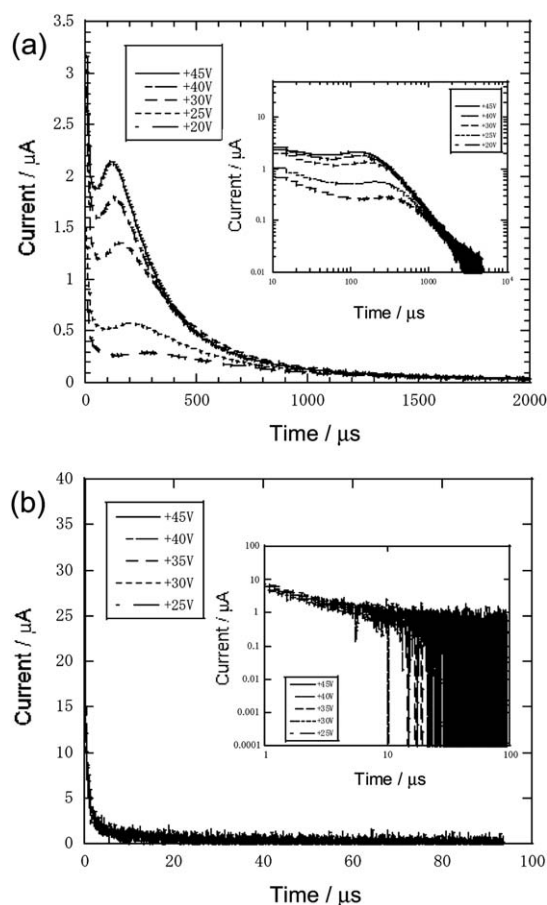


Fig. 6 Transient photocurrents of holes (a) in the SmB_{hex} glassy phase (55 °C); (b) in the polycrystalline phase (55 °C), of LCG-triester 8-PNP-O12 in a 15 μm thick glass cell pre-coated by an ITO electrode at various applied voltages. The inset shows the double logarithmic plot of respective transient photocurrents as a function of time.

Table 1 Hole mobility of LCG-triester 8-PNP-O12 in different phases

Phase	Hole mobility cm ⁻² v ⁻¹ s ⁻¹ (at 25 V)
SmA	1.25 × 10 ⁻⁴
SmB _{hex}	5 × 10 ⁻⁴
SmB _{hex} glass	3.5 × 10 ⁻⁴
Polycrystal	—

SmB_{hex} phase. Each photocurrent is also non-dispersive and shows a clear shoulder. The hole mobility is estimated to be 3.5 × 10⁻⁴ cm² V⁻¹ s⁻¹ at 25 V. This mobility is almost the same as that in SmB_{hex} phase, indicating that the charge transport properties of the SmB phase are successfully maintained in solid state, *i.e.*, glassy SmB_{hex} phase.

On the other hand, the transient photocurrents in the polycrystalline phase decay rapidly as shown in Fig. 6(b). It indicates that there are lots of defects or deep trap states in the bulk to stop the carrier transport, which are possibly caused by grain boundaries among the polycrystallites. Therefore, the carrier transport properties were dramatically decreased in the polycrystal phase. We summarize the charge carrier transport properties of LCG-triester 8-PNP-O12 in Table 1.

As for the mobility in liquid crystal glass states, the relatively high OFET mobility of 10⁻² cm² v⁻¹ s⁻¹ was reported in the nematic glassy phase of oligofluorene derivatives.³⁴ However, we might expect higher mobility up to 0.1 cm² v⁻¹ s⁻¹ or more if highly ordered smectic mesophases were turned to glass, because the charge carrier mobility in smectic mesophases depends on molecular order in a smectic layer, as reported previously.³⁵

The fixation of molecular motion in liquid crystalline phases is one of continuous interest for device applications of liquid crystalline organic semiconductors. In fact, various approaches have been proposed, which include reactive mesogens with polymerizable function groups,³⁶ immobile liquid crystalline composites with a cross-linker,³⁷ polymeric liquid crystals,³⁸ and dried lyotropic liquid crystals reported more recently.³⁹ Utilization of the LC-glass is another approach, as demonstrated in nematic and discotic glasses.^{26,34}

Conclusions

In this study, we have successfully prepared a novel smectic glass, 1,3,5-benzenetricarboxylic acid, tris{12-[6'-(4''-octylphenyl)-2'-naphthylxy]-1-dodecyl ester} containing a mesogenic 2-phenylnaphthalene moiety. This material exhibited SmA and SmB_{hex} phases when cooled from an isotropic phase at slow cooling rates, but exhibited a glassy SmB_{hex} phase when cooled at high cooling rates. This is the first reported case of the glass state of the SmB_{hex} phase in small molecules, whose glass transition temperature, *T*_g was as high as 60 °C. We also report for the first time, the charge carrier transport properties in smectic liquid crystal glassy phases: the highest charge carrier transport mobility in the SmB_{hex} glass phase was around 3.5 × 10⁻⁴ cm² V⁻¹ s⁻¹ for holes, which is comparable to that for the SmB_{hex} phase. In addition, the mobility in the SmB_{hex} glassy phase depends on the temperature, but not on the electric field, which is quite different from amorphous materials. The details will be

reported elsewhere soon. These properties indicate that the smectic liquid crystal glass provides us with solid self-organized molecular aggregates while keeping easy control over the molecular alignment in smectic liquid crystals, which shows promising advantages over both amorphous and crystalline materials as a new type of organic semiconductors.

Acknowledgements

The authors would like to thank Dr Hiroaki Iino and Dr Akira Ohno for helpful discussions regarding experimental analysis, and to thank Center for Advanced Materials Analysis (Suzuka-kedai), Technical Department, Tokyo Institute of Technology, for MS analysis. The authors are also grateful for the financial supports from a Core Research for Evolutional Science and Technology (CREST) program sponsored by Japan Science and Technology Agency.

Notes and references

- P. M. Borsenberger and D. S. Weiss, *Organic photoconductors for Imaging System*, Marcel Dekker, New York, 1993.
- C. W. Tang and S. A. van Slyke, *Appl. Phys. Lett.*, 1987, **51**, 12.
- M. van der Auweraer, F. C. Schryver, P. M. Borsenberger and H. Bässler, *Adv. Mater.*, 1994, **6**, 199.
- H. Bässler, *Phys. Status Solidi B*, 1993, **175**, 15.
- J. Mort and A. I. Lakatis, *J. Non-Cryst. Solids*, 1970, **4**, 117.
- R. G. Kepler, *Phys. Rev.*, 1960, **119**, 1226.
- E. A. Silinsh, *Organic Molecular Crystals*, 1980, Springer, Berlin.
- M. Yamashita and Y. Amemiya, *Jpn. J. Appl. Phys.*, 1978, **17**, 1513.
- K. Okamoto, S. Nakajima, A. Itaya and Kusabayashi, *Bull. Chem. Soc. Jpn.*, 1983, **56**, 3930.
- B. Blanzat, C. Barthou, N. Tercier, J.-J. André and J. Simon, *J. Am. Chem. Soc.*, 1987, **109**, 6193.
- N. Boden, R. J. Bushby, J. Clements, M. V. Jesudason, P. F. Knowles and G. Williams, *Chem. Phys. Lett.*, 1988, **152**, 94.
- A. Belarbi, M. Maitrot, K. Ohta, J. Simon, J. J. André and P. Petit, *Chem. Phys. Lett.*, 1988, **143**, 400.
- P. G. Schouten, J. M. Warman, M. P. de Haas, M. A. Fox and H.-L. Pan, *Nature*, 1991, **252**, 736.
- P. G. Schouten, J. M. Warman, M. P. de Haas, J. F. van der Pol and J. W. Zwikker, *J. Am. Chem. Soc.*, 1992, **114**, 9028.
- J. Wu, T. Usui, A. Ohno and J. Hanna, *Chem. Lett.*, 2009, **38**, 592.
- G. B. Vaughan, P. A. Heiney, J. P. MacCauley and A. B. Smith III, *Phys. Rev. B: Condens. Matter*, 1992, **46**, 2788.
- D. Adam, F. Closs, T. Frey, D. Funhoff, D. Haarer, H. Ringsdorf, P. Schuhmacher and K. Siemensmeyer, *Phys. Rev. Lett.*, 1993, **70**, 457.
- D. Adam, P. Schuhmacher, J. Simmerer, L. Häussling, K. Siemensmeyer, K. H. Etzbach, H. Ringsdorf and D. Haarer, *Nature*, 1994, **371**, 141.
- L. L. Chapoy, D. K. Munck, K. H. Rasmussen, E. J. Diekmann, R. K. Sethi and D. Biddle, *Mol. Cryst. Liq. Cryst.*, 1984, **105**, 353.
- M. Funahashi and J. Hanna, *Appl. Phys. Lett.*, 2000, **76**, 2574.
- J. Hanna, *Opto-Electron. Rev.*, 2005, **13**, 259.
- I. K. Iverson, S. M. Casey, W. Seo and S. W. T. Chang, *Langmuir*, 2002, **18**, 3510.
- H. Maeda, M. Funahashi and J. Hanna, *Mol. Cryst. Liq. Cryst.*, 2000, **346**, 183.
- M. Funahashi and J. Hanna, *Phys. Rev. Lett.*, 1997, **78**, 2184.
- K. Tokunaga, H. Iino and J. Hanna, *J. Phys. Chem. B*, 2007, **111**, 12041.
- D. Adam, P. Schuhmacher, J. Simmerer, L. Häussling, W. Paulus, K. Siemensmeyer, K. H. Etzbach, H. Ringsdorf and D. Haarer, *Adv. Mater.*, 1995, **7**, 276.
- F. Fan, S. W. Culligan, J. Mastrangelo, D. Katsis and S. H. Chen, *Chem. Mater.*, 2001, **13**, 4584.
- K. Yonetake, O. Haba and T. Takahashi, *Jpn. Kokai Tokkyo Koho*, 2008, JP 2008239987.
- N. Miyaura and A. Suzuki, *Chem. Rev.*, 1995, **95**, 2457.

- 30 M. Funahashi and J. Hanna, *Appl. Phys. Lett.*, 1997, **71**, 602.
- 31 S. H. Chen, J. C. Mastrangelo, H. Q. Shi, T. N. Blanton and A. B. Hashemi, *Macromolecules*, 1997, **30**, 93.
- 32 H. Ahn, A. Ohno and J. Hanna, *Jpn. J. Appl. Phys.*, 2005, **44**, 3764.
- 33 H. Ahn, A. Ohno and J. Hanna, *J. Appl. Phys.*, 2007, **102**, 093718.
- 34 T. Yasuda, K. Fujita, T. Tsutsui, Y. Geng, S. W. Culligan and S. H. Chen, *Chem. Mater.*, 2005, **17**, 264.
- 35 M. Funahashi and J. Hanna, *Appl. Phys. Lett.*, 1998, **73**, 3733.
- 36 T. Kreouzis, R. J. Baldwin, M. Shkunov, I. McCulloch, M. Heeney and W. Zhang, *Appl. Phys. Lett.*, 2005, **87**, 172110.
- 37 N. Yoshimoto and J. Hanna, *Adv. Mater.*, 2002, **14**, 988.
- 38 H. Sirringhaus, R. J. Wilson, R. H. Friend, M. Inbasekaran, W. Wu, E. P. Woo, M. Grell and D. D. C. Bradley, *Appl. Phys. Lett.*, 2000, **77**, 406.
- 39 V. G. Nazarenko, O. P. Boiko, M. I. Anisimov, A. K. Kadashchuk, Yu. A. Nastishin, A. B. Golovin and O. D. Lavrentovich, *Appl. Phys. Lett.*, 2010, **97**, 263305.